Am J Cancer Res 2020;10(3):925-938
www.ajcr.us /ISSN:2156-6976/ajcr0102830

Original Article

N-terminal truncated carboxypeptidase E represses E-cadherin expression in lung cancer by stabilizing the Snail-HDAC complex

Jing Sun[1*], Dawei Meng[3*], Tao Yu[4*], Feng Li[5,6], Guirong Zhang[1], Xin Tian[7], Nannan Zhao[4], Guimin Li[3], Lu Li[8], Hongyue Wang[9], Yeqiu Liu[4], Yiming Meng[1], Yushu Ma[1], Zhong Wan[9], Jimin Bao[3], Haozhe Piao[1,2]

[1]Central Laboratory, Cancer Hospital of China Medical University, Liaoning Cancer Hospital & Institute, Shenyang 110042, Liaoning, China; [2]Department of Neurosurgery, Cancer Hospital of China Medical University, Liaoning Cancer Hospital & Institute, Shenyang 110042, Liaoning, China; [3]Department of Otolaryngology Head and Neck Surgery, Liaoning Provincial Jinqiu Hospital, Shenyang 110016, Liaoning, China; [4]Department of Medical Imaging, Cancer Hospital of China Medical University, Liaoning Cancer Hospital & Institute, Shenyang 110042, Liaoning, China; [5]Department of Cell Biology, Key Laboratory of Cell Biology, Ministry of Public Health of The PRC, China Medical University, Shenyang 110122, Liaoning, China; [6]Key Laboratory of Medical Cell Biology, Ministry of Education of The PRC, China Medical University, Shenyang 110122, Liaoning, China; [7]Molecular Oncology Laboratory of Cancer Research Institute, China Medical University First Hospital, Shenyang 110001, Liaoning, China; [8]Research Center of Translational Medicine, The Second Affiliated Hospital of Shantou University Medical College, Shantou 515000, Guangdong, China; [9]Department of Scientific Research and Academic, Cancer Hospital of China Medical University, Liaoning Cancer Hospital & Institute, Shenyang 110042, Liaoning, China. [*]Co-first authors.

Received September 26, 2019; Accepted December 16, 2019; Epub March 1, 2020; Published March 15, 2020

Abstract: The N-terminal truncated carboxypeptidase E (CPEΔN) protein, an alternative splicing product of the carboxypeptidase E gene, has recently been recognized as an independent predictor for the recurrence and metastasis of lung adenocarcinoma. In this study, we showed that CPEΔN may accelerate lung cancer invasion via an E-cadherin-dependent mechanism. *In vitro* experiments and *in vivo* bioluminescence imaging assay revealed CPEΔN promoted the mobility and invasion of human lung cancer cells by suppressing endogenous expression of E-cadherin, a critical regulator for epithelial tissue homeostasis. Further mechanistic analyses revealed that CPEΔN directly interacted with and stabilized the Snail/HDAC1/HDAC3 complex within the promoter region of the E-cadherin-encoding *CDH1* gene. CPEΔN overexpression led to a reduction of histone H3K9 acetylation and an increase of H3K9 and H3K27 trimethylation in the *CHD1* gene promoter and ultimately inhibited E-cadherin transcription. In addition, correlations among CPEΔN, E-cadherin expression and tumor progression in 195 cases of lung adenocarcinoma patients were analyzed. Higher nuclear expression of CPEΔN was detected in patients with advanced stage of lung adenocarcinoma. Nuclear expression of CPEΔN was negatively correlated with the cell membrane expression of E-cadherin. Collectively, our findings illustrated that CPEΔN was involved in the transcriptional regulation of the epithelial-mesenchymal transition-related gene *CDH1* and provide novel insights into CPEΔN-associated lung cancer metastasis.

Keywords: N-terminal truncated carboxypeptidase E, lung adenocarcinoma, recurrence, metastasis, epithelial-mesenchymal transition, E-cadherin, epigenetic modification, Snail/HDAC1/HDAC3 complex, transcription regulation

Introduction

Lung cancer is a malignancy with high morbidity and mortality. Approximately 1.2 million patients worldwide die from lung cancer each year [1], and relapse and metastasis are the major causes of death in most patients. Once diagnosed, the 5-year survival rate is lower than 15% [2]. Therefore, exploring molecular diagnostic indicators for predicting the metastatic potential of lung cancer is of great significance and clinical value.

Carboxypeptidase E (CPE) is a metal ion-dependent endopeptidase primarily expressed in endocrine or neuroendocrine cells and usually

exists in either a membrane-bound or soluble form [3-5]. CPE not only cleaves C-terminal amino acid residues to generate mature hormones or neuropeptides [6], but also functions as a neurotrophic factor to promote neuronal survival, independent of its peptidase activity [7]. Recently, a novel selective splicing product of CPE was discovered, named CPEΔN, which lacks the first N-terminal 35 aa. Several studies showed that CPEΔN functions as an independent prognostic indicator for recurrence and metastasis of hepatocellular carcinoma, lung cancer and colorectal cancer [8-10]. Lee et al found that CPEΔN was mainly distributed in the nuclei of hepatocytes and breast cancer and colorectal cancer cell lines. The metastasis-related proteins neural precursor cell expressed, developmentally down-regulated 9 (NEDD9) and matrix metallopeptidase 9 (MMP9) were increased with CPEΔN overexpression in hepatocyte cell lines, and CPEΔN was shown to bind histone deacetylases HDAC1 and HDAC2 [8]. Skalka et al reported that both full-length CPE and CPEΔN were involved in the WNT/β-catenin pathway; full-length CPE inhibits WNT signaling, while CPEΔN positively regulates the WNT pathway [11]. Our research group confirmed that both full-length CPE and CPEΔN were detectable in lung adenocarcinoma tissue, and high expression of CPEΔN was associated with poor prognosis in lung adenocarcinoma [9]. These findings illustrated that the mechanism that CPEΔN promoted tumor recurrence and metastasis is indistinct.

E-cadherin, encoded by the *CDH1* gene, is a calcium-dependent cell-cell adhesion protein. E-cadherin forms scaffold structures with β-catenin, γ-catenin, α-catenin and actin through its cytoplasmic region to stabilize cell adhesion linkages and inhibit cancer cell migration [12, 13]. Mutation, post-transcription modifications and many other factors can affect the function of E-cadherin to contribute to cancer progression by increasing proliferation, invasion or metastasis [14, 15]. Snail is a transcriptional repressor that downregulates target gene expression by sequence-specific DNA binding. Snail recruits HDAC1/HDAC2 and the methyltransferase EZH2 to the *CDH1* promoter region, resulting in weakened acetylation and increased trimethylation at Lys-9 and Lys-27 of histone 3 (H3K9 and H3K27) in the *CDH1* promoter, causing reduced transcription of *CDH1* gene [16, 17].

In the present study, we confirmed that CPEΔN binds to the *CDH1* promoter, stabilizes the Snail/HDAC/EZH2 complex, and represses *CDH1* transcription and expression by promoting the switch between histone H3K9 and H3K27 acetylation and trimethylation. These results show that CPEΔN acts as a transcriptional regulator for the *CDH1* gene, which provides a new molecular mechanism of CPEΔN in promoting lung cancer metastasis.

Materials and methods

Cell culture

All cell lines were purchased from ATCC or Chinese Academy of Sciences Cell Bank. Cell culture, migration and invasion assays are described in Supplementary Materials and Methods. All experiments were performed with mycoplasma-free cells.

Real-time PCR and western blotting

See Supplementary Materials and Methods for details.

Construction of expression vectors.

See Supplementary Materials and Methods for details.

Establishment of metastatic animal models with CPEΔN-overexpressing cells

The human CPEΔN gene was cloned into the pLenti-Luc vector (Obio Technology, Shanghai, China). H1299 cells transduced with pLenti-CPEΔN or control lentiviral vectors were selected with 2 μg/mL puromycin. BALB/c nude mice were divided into two groups (10 mice in each group). CPEΔN-H1299 or control H1299 cell suspensions (2×10^6) were injected into the lateral tail vein of 4- to 6-week-old nude mice. Tumor metastases were monitored every two weeks after tail vein injection by the IVIS@ Lumina II system (Caliper Life Sciences, Hopkinton, MA, USA).

Coimmunoprecipitation

Cells were harvested and lysed in lysis buffer (0.5 NP-40, 50 mM Tris, 100 mM NaCl, 1 mM EDTA, 1 mM Na_3VO_4, 50 mM NaF and 1 mM β-mercaptoethanol), supplemented with Roche protease inhibitor cocktail. Lysis buffer (800 μl)

and antibody (1-2 mg) were added, after gentle vortexing, the beads were incubated for 3 to 5 h, and Protein A/G Sepharose beads were added (GE Healthcare) and incubated for 6 h. NETN lysis buffer (150 mM NaCl, 1 mM EDTA, 50 mM Tris-HCl, 1 NP-40, 1 mM phenylmethylsulfonyl fluoride, 0.5 mg/ml leupeptin and 0.5 mg/ml pepstatin) was used for washes at least three, and the respective antibody was used for immunoprecipitation.

GST pull-down assay

The CPEΔN coding sequence was inserted into the pGEX-4T-1 vector (Amersham). The GST-CPEΔN fusion protein (approximately 70 kDa) was produced in *E. coli* JM109 and purified The HDAC1, HDAC3, EZH2 and Snail genes were inserted into the pET-28a vector (Novagen). His 60 Ni Superflow Resin (TaKaRa) was used to purify His-tagged proteins according to standard procedures. The GST-CPEΔN protein was bound to glutathione Spheres 4B beads (Amersham Biosciences). Purified His-tagged target protein was added to the GST-CPEΔN sample, and beads were incubated for 8 h. GST-binding buffer (100 mM NaCl, 50 mM NaF, 2 mM EDTA, 1 NP-40 and protease inhibitor mixture) was used to wash the resin at least three times before immunoblotting.

Chromatin immunoprecipitation

The EZ-Zyme™ Chromatin Immunoprecipitation Kit (Millipore; #17-371 and #17-375) was used according to the manufacturer's instructions. Cell lysates (200 μg protein) were used for immunoprecipitation reactions with anti-CPE (BD #610758), anti-Snail (#sc10432, Santa Cruz), anti-HDAC1 (#ab7028, Abcam), anti-HDAC3 (#ab7030, Abcam), anti-EZH2 (#17-662, Millipore), anti-H3K4Me3 (#Ab12209, Abcam), anti-H3K36Me3 (#Ab9050, Abcam), anti-H3K27M3 (#ab92985, Abcam), anti-H3K9M3 (#ab176916, Abcam), Anti-H3K27Ac (#ab45173, Abcam), anti-H3K9Ac (#ab32129, Abcam) or normal IgG. Precipitated genomic DNA was amplified by real-time PCR with primers for the *CDH1* promoter. Percentage enrichment over input chromatin was determined. Each ChIP assay was repeated at least twice, and representative data are presented.

The PCR primers are shown in Supplementary Table 4. ChIP primer 1 was used to amplify the E-box-1-2 region of the *CDH1* promoter, and ChIP primer 2 was used to amplify the E-box-2-3 region of the *CDH1* promoter. Primer 2 was used to perform real-time PCR after the ChIP assay.

RNA interference

See Supplementary Materials and Methods for details.

Immunohistochemical (IHC) staining

We performed IHC staining of CPE and E-cadherin in lung adenocarcinoma and hepatocellular carcinoma samples. Tissue microarrays with 75 lung adenocarcinomas and 205 hepatocellular carcinomas were purchased from Xinchao Biochip Company Ltd, Shanghai, China (HLugAde150Sur01 and LV2161). Paraffin-embedded sections were prepared from surgical specimens of lung adenocarcinoma in Liaoning Cancer Hospital from February 2012 to December 2014. Immunohistochemistry was performed according to a previously reported method [34]. Samples were incubated with antibodies against CPE (LS-B9256; 1:50 dilution) and E-cadherin (#610182; 1:100, BD Biosciences) at 4°C for 18 h. Samples were scored using a semi-quantitative scoring system that is widely used in Germany. Samples were first scored for staining intensity (0, no staining; 1, light yellow; 2, pale brown; 3, brown). A second score was given according to the ratio of stained cells (0, 0-5; 1, 5-25; 2, 25-50; 3, >50). The final score was determined as the product of both scores and ranged from 0 (minimum) to 12 (maximum). A CPE staining score ≤6 was defined as low CPE expression, while a score >6 indicated high CPE expression. For cell membrane expression of E-cadherin, a score ≤1 was defined as low, and a score >1 indicated high membrane expression. Immunological staining was scored by a pathologist double blinded for specimen source and prognosis.

Statistical analysis

Statistical analysis was performed by SPSS version 20.0 software (SPSS Inc. Chicago, IL, USA). All experimental data were expressed as mean ± standard deviation (SD) and were assessed by Student's t-test. Scores were compared by the chi-square test. The correlation

between nuclear CPE expression and membrane E-cadherin levels was determined by Pearson's correlation. P<0.05 was considered to indicate statistical significance.

Results

CPEΔN enhances lung cancer cell migration and invasion

Our previous study showed that high expression of CPEΔN, the 40 kDa truncated form of CPE, is a predictor of poor prognosis in lung adenocarcinoma. To examine the potential molecular mechanisms of CPEΔN in lung cancer recurrence, we first analyzed the expression of full-length CPE and CPEΔN in lung, colon, breast, and head and neck cancer cell lines. All tumor cell lines except the breast cancer MDA-MB-231 cell line expressed only CPEΔN (**Figure 1A** and Supplementary Figure 1). CPEΔN expression levels in the highly metastatic 95D and H1395 cell lines were higher than those in the low metastatic H1299 and H292 lung cancer cell lines.

To determine whether CPEΔN promotes migration and infiltration in lung cancer cells, CPEΔN was knocked down in 95D cells using three siRNAs (**Figure 1B**). SiCPEΔN1 and SiCPEΔN3 yielded similar knockdown efficiency and both were used in subsequent experiments. Wound healing and transwell assays were used to evaluate the role of CPEΔN in cell migration. The results showed that CPEΔN knockdown in 95D lung cancer cells significantly reduced cell migration and invasion compared with controls (P<0.05) (**Figure 1C** and **1D**).

Next, CPEΔN was overexpressed in H1299 cells, which show low endogenous expression of CPEΔN. The amounts of transfected plasmid were optimized to obtain expression of CPEΔN similar to levels in 95D cells (Supplementary Figure 2). CPEΔN overexpression resulted in increased invasion ability compared with control cells in transwell assays (**Figure 1D** and **1E**). Together with knockdown experiments, these findings indicated that CPEΔN expression enhances mobility and invasion in lung cancer cells *in vitro*.

To further evaluate the effect of CPEΔN on tumor cell metastasis and invasion, we performed mouse xenograft experiments with a luciferase-expressing CPEΔN-H1299 cell clone or control H1299 cells by tail vein injection. The tumors were detected by *in vivo* bioluminescence imaging. Two weeks after injection, tumors were detected in the lung, thyroid, ilium, humerus and testis in five of ten mice in the CPEΔN-H1299 group, but only in the bilateral iliac bone of one mouse in the control H1299 group (**Figure 1H**). Luciferase activity peaked at 6 weeks after inoculation and was 12 times higher in the CPEΔN-H1299 group relative to the control H1299 group (**Figure 1G**). The *in vitro* and *in vivo* metastasis analyses supported the conclusion that CPEΔN enhances migration and invasion in lung cancer cell lines.

CPEΔN downregulates the expression of E-cadherin in lung cancer cell lines

Multiple studies have shown that cancer cell metastatic ability is regulated by the network of EMT-related proteins, including E-cadherin, α-catenin, β-catenin and γ-catenin [13]. To explore the molecular mechanism by which CPEΔN promotes migration in lung cancer cells, we analyzed the gene and protein expressions of the E-cadherin-catenin adhesion complex by qPCR and western blot. As shown in **Figure 2A** and **2B**, E-cadherin expression at both mRNA and protein levels was significantly increased in CPEΔN-knockdown 95D cells compared with controls, while α-catenin, β-catenin and γ-catenin protein levels were not affected. We also overexpressed CPEΔN in H1299 cells, which have low expression of endogenous CPEΔN. Overexpression of CPEΔN resulted in reduced E-cadherin mRNA and protein levels, which was consistent with the knockdown results (**Figure 2A** and **2B**).

To explore whether downregulation of E-cadherin is necessary for CPEΔN-associated cancer cell invasion, we performed a rescue experiment. We transfected the E-cadherin plasmid into 95D cells transfected with control RNAi and confirmed similar levels of E-cadherin in the control RNAi cells compared with siCPEΔN cells (**Figure 2C**). Transwell assays showed that introduction of E-cadherin into control RNAi-transfected cells reduced cell migration to levels similar to the siCPEΔN group (**Figure 2C**). These results indicate that CPEΔN promotes cancer invasion by repressing E-cadherin and that E-cadherin down-regulation is necessary for CPEΔN-mediated induction of invasion.

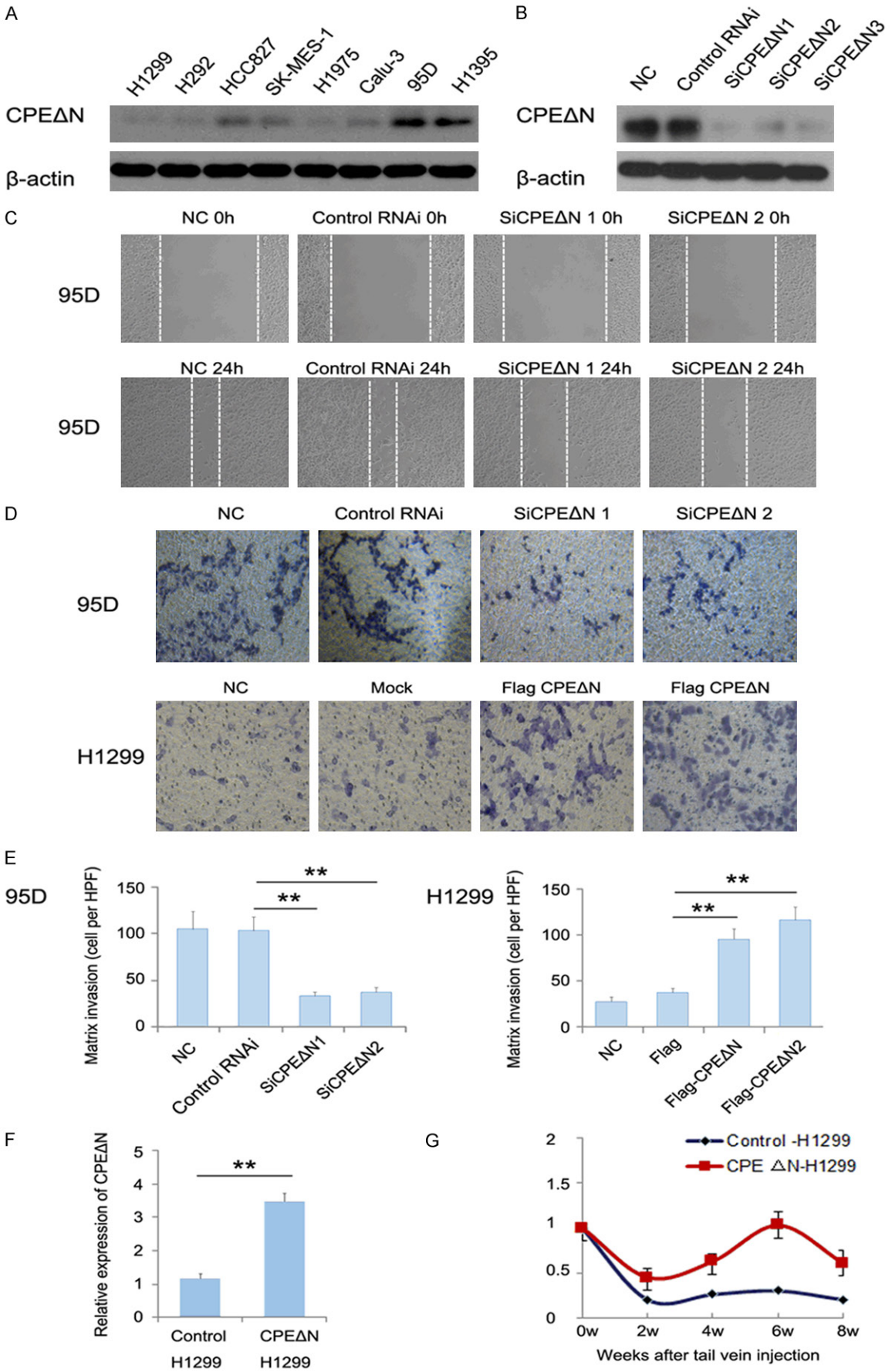
A
H1299
H292
HCC827
SK-MES-1
H1975
Calu-3
95D
H1395
CPEΔN
β-actin
B
NC
Control RNAi
SiCPEΔN1
SiCPEΔN2
SiCPEΔN3
CPEΔN
β-actin
C
NC 0h
Control RNAi 0h
SiCPEΔN 1 0h
SiCPEΔN 2 0h
95D
NC 24h
Control RNAi 24h
SiCPEΔN 1 24h
SiCPEΔN 2 24h
95D
D
NC
Control RNAi
SiCPEΔN 1
SiCPEΔN 2
95D
NC
Mock
Flag CPEΔN
Flag CPEΔN
H1299
E
95D
Matrix invasion (cell per HPF)
150
100
50
0
**
**
NC
Control RNAi
SiCPEΔN1
SiCPEΔN2
H1299
Matrix invasion (cell per HPF)
150
100
50
0
**
**
NC
Flag
Flag-CPEΔN
Flag-CPEΔN2
F
Relative expression of CPEΔN
5
4
3
2
1
0
**
Control H1299
CPEΔN H1299
G
Control -H1299
CPE △N-H1299
2
1.5
1
0.5
0
0w
2w
4w
6w
8w
Weeks after tail vein injection

H

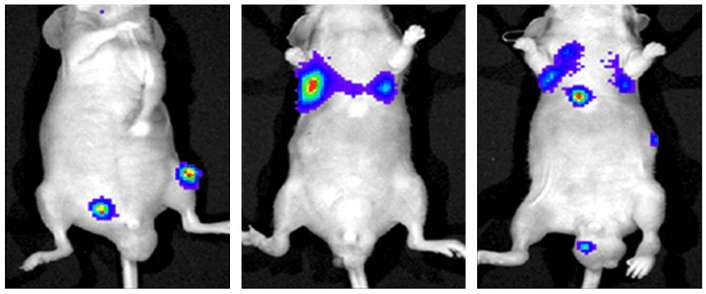

Figure 1. CPEΔN enhances lung cancer cell invasion and metastasis. (A) CPEΔN protein levels were detected examined in eight lung cancer cell lines by western blotting. (B) 95D lung cancer cells were transfected with three different CPEΔN siRNAs or control siRNA. After 24 h, CPEΔN protein was analyzed by western blotting. (C) 95D lung cancer cells were transfected with control siRNA, siCPEΔN1 or siCPEΔN2, untreated cells were used as additional control. At 48 h after transfection, a scratch was made in the cell monolayer and photos were acquired after 0 and 24 h. (D and E) In vitro cell migration and invasion assays were performed in transwell plates. Top row, 95D cells were transfected as described in (C). Bottom, H1299 cells transfected with empty vector or FLAG-CPEΔN plasmid. After 48 h, cells were seeded at 5×10^5 per well and induced to invade through Matrigel-coated membranes for 24 h. The membranes were then fixed and imaged (D) and data were quantified (E). Representative results from three independent experiments are shown. (F) The pLenti-CPEΔN expression vector or control lentivirus construct was transfected into the H1299 cell line, and stable cell lines were established. The expression of CPEΔN was analyzed by western blotting and grayscale quantitation. (G) CPEΔN-H1299 or control H1299 cells were injected into the lateral tail vein of 4-6-week-old BALB/c nude mice (n=10 each group). Tumor metastases were monitored at every two weeks after tail vein injection. Relative luciferase signals data (mean ± standard deviation) was captured at 0, 2, 4, 6, and 8 weeks. (H) Representative images of mice at 2 weeks after tail vein injection with control H1299 or CPEΔN H1299 cells. *indicates significant difference ($P<0.05$), **indicates significant difference ($P<0.01$).

CPEΔN binds to the CDH1 gene promoter and represses CDH1 expression

HDAC1 and HDAC2 are histone deacetylases that remove histone acetylation to inhibit gene transcription [18]. A recent study reported that CPEΔN directly interacts with HDAC1 and HDAC2 [8]. To test whether CPEΔN is involved in histone modification in the *CDH1* gene promoter and therefore inhibits gene transcription, we examined whether CPEΔN interacted with the E-box-1-2 and E-box-2-3 regions of the *CDH1* promoter using chromatin immunoprecipitation with anti-CPEΔN antibody. E-box-2-3 region of CDH1, but not the 1-2 E-Box region, was amplified in CPEΔN-H1299 cells (**Figure 3A** and **3B**). The E-box-2-3 region is a classical binding region for transcriptional regulators, such as Snail and TWIST1 [16]. We next analyzed trimethyl and acetylated modifications at Lys-9, Lys-27, Lys-4 and Lys-36 of histone 3, which are transcriptional inhibition or activation modifications [19]. ChIP-PCR experiments showed that the overexpression of CPEΔN induced significantly higher levels of H3K27 and H3K9 trimethylation ($P<0.05$) and reduced H3K9 acetylation compared with controls, while no differences in H3K27Ac were observed (**Figure 3C** and **3D**). These findings suggest that CPEΔN may bind to the *CDH1* promoter region and affect histone modifications.

CPEΔN interacts with HDAC1, HDAC3, Snail and EZH2

To further elucidate the molecular basis of CPEΔN in regulating the transcription of *CDH1*, nuclear extracts of CPEΔN-H1299 cells were immunoprecipitated using CPE antibody and the interacting proteins were identified by mass spectrometry. As shown in Supplementary Table 1, RNA polymerase II big subunits, several hypothetical methyltransferases and SPT5/SPT4, components of the DRB sensitivity-inducing factor complex that regulates transcription elongation by RNA polymerase II [20-24], were precipitated by CPEΔN. These results indicate that CPEΔN may function in transcriptional regulation by interacting with transcriptional regulators.

Based on these data, we analyzed the binding between CPEΔN and well-known transcriptional regulators of *CDH1*, such as Snail, Slug, HDACs, SUZ12 and EZH2 [25-28], using co-immunoprecipitation. The results showed that CPEΔN interacted with Snail, HDAC1, HDAC3 and EZH2, but not with Slug, HDAC2 or SUZ12,

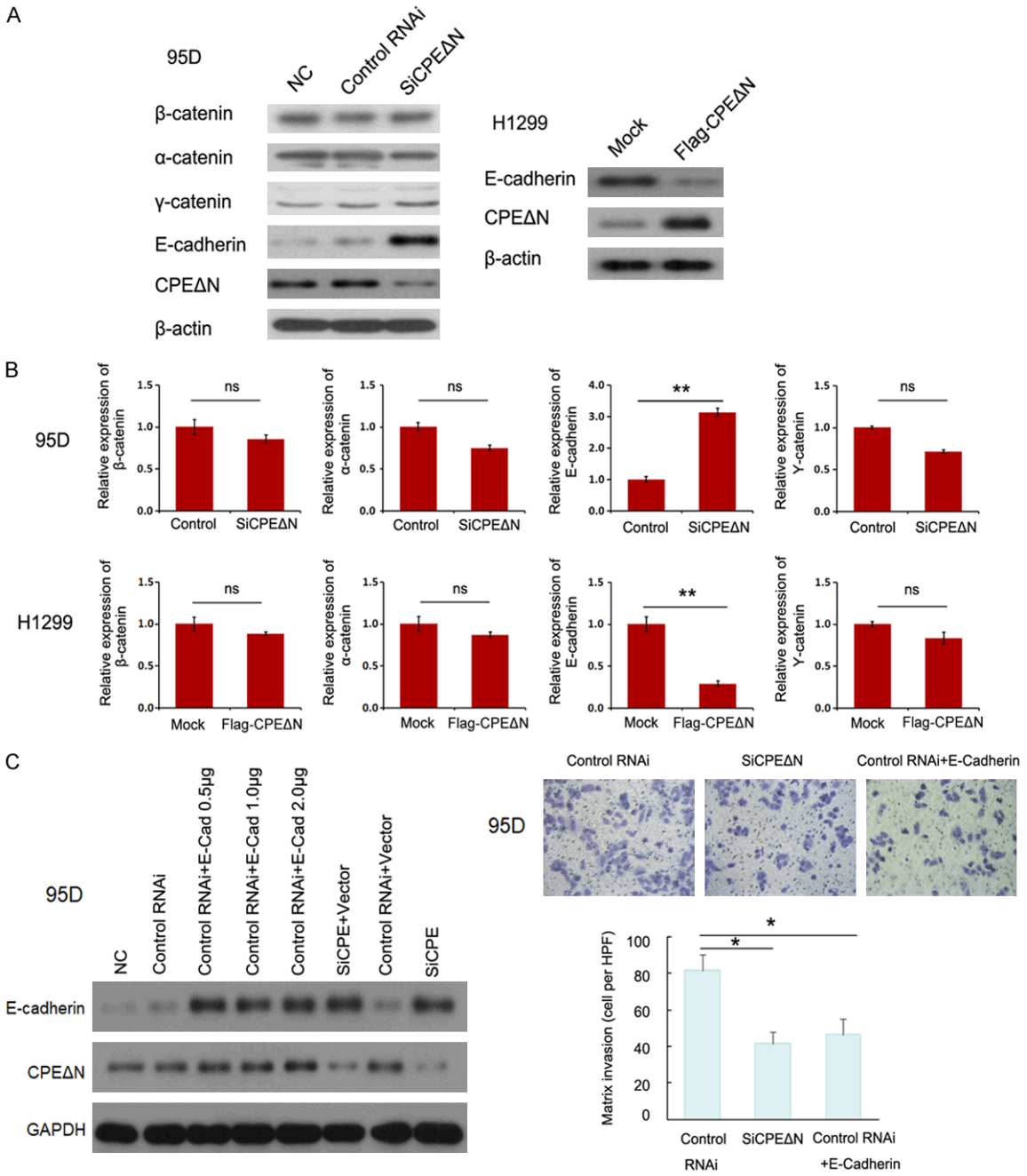

Figure 2. CPEΔN downregulates the adhesion related protein E-cadherin. A. Left, 95D cells were transfected with control siRNA or siCPEΔN; after 48 h, the expression levels of adhesion-related proteins E-cadherin, α-catenin, β-catenin and γ-catenin were assessed by western blotting. Right, control vector or FLAG-CPEΔN was transfected into H1299 cells; after 24 h, the expressions of E-cadherin and CPEΔN were detected. B. The effects of CPEΔN on the transcription of E-cadherin, α-catenin, β-catenin and γ-catenin genes were analyzed by real time PCR; representative results from three independent experiments are shown. Data were analyzed by Student's t-test. Top, 95D cells were transfected with control siRNA or siCPEΔN. Bottom, H1299 cells were transfected with vector or FLAG-CPEΔN. C. 95D lung cancer cells were divided into control siRNA, siCPEΔN or control siRNA+E-cadherin groups; at 48 h after transfection, the cells were seeded at 5×10^5 per well. The cells were induced to invade through Matrigel-coated membranes for 24 h. The membranes were fixed, imaged (top) and quantitated (bottom). The protein expression levels of CPEΔN and E-cadherin were analyzed by western blotting, GADPH was used an internal control (left).

in the high CPEΔN expressing 95D and H1395 cells (**Figure 4A**). To detect direct physical interactions between CPEΔN with Snail, HDAC1, HDAC3 and EZH2, pull-down assays were per-

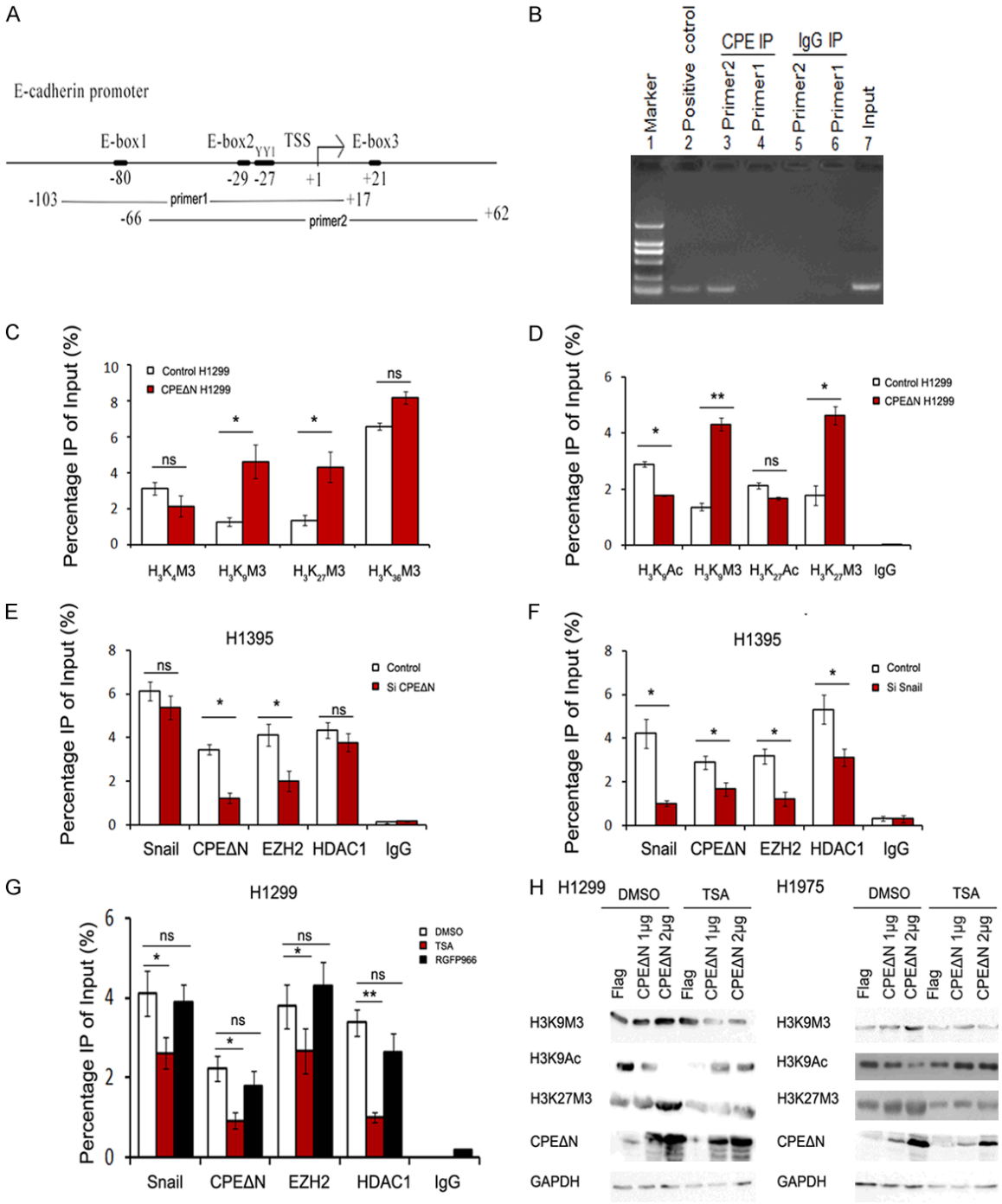

Figure 3. CPEΔN binds to the *CDH1* promoter and represses *CDH1* transcription. A. ChIP PCR primer corresponded to the *CDH1* promoter region was described. B. ChIP assays were performed in 95D cells using anti-CPE antibody; binding of CPEΔN to the *CDH1* promoter was analyzed by real-time PCR, with amplification products resolved by 2% agarose gel electrophoresis. C. ChIP and real time PCR assays were carried out with antibodies against H3K9M3, H3K27M3, H3K4M3 and H3K36M3 in control-H1299 and CPEΔN-H1299 cells; D. ChIP-PCR assays were performed in control-H1299 and CPEΔN-H1299 cells using antibodies against H3K9M3, H3K9AC, H3K27M3 and H3K27AC. E. H1395 cells were transfected with control siRNA or siCPE; after 48 h, CPE, HDAC1, Snail and EZH2 antibodies were used for ChIP assay and real time PCR. F. H1395 cells were transfected with control siRNA or siSnail for 48 h; CPE, HDAC1, Snail and EZH2 antibodies were used for ChIP and real time PCR. G. CPEΔN-H1299 cells were treated with DMSO, 300 nM TSA or 10 μM RGFP966 for 24 h; antibodies targeting CPEΔN, HDAC1, Snail, and EZH2 were used to perform ChIP-PCR assays. Binding of proteins to the *CDH1* promoter region was evaluated. H. H1975 and H1299 cells with low CPEΔN expression were transfected with the vector and increasing amounts of CPEΔN plasmid; after

24 h, DMSO or 300 nM TSA was added for 12 h. Western blot was used to analyze the protein expression levels of H3K9M3, H3K27M3, and H3K9AC, with GAPDH as a loading control.

formed with bacterially expressed and purified proteins. We found that CPEΔN directly interacted with HDAC1, HDAC3 and Snail, while no direct interaction was detected between CPEΔN and EZH2 (**Figure 4B**). These results suggest that the interaction between CPEΔN and EZH2 detected by co-immunoprecipitation may be mediated by Snail and/or HDAC1/3.

Next, we sought to identify the key molecule that recruits EZH2 to the CPEΔN/HDAC1/HDAC3/Snail complex. HDAC1, HDAC3 and Snail were separately knocked down by siRNA in H1395 cells with more than 70% knock down efficiency (**Figure 4C**). HDAC1 and HDAC3 knockdown did not alter the interaction between EZH2 and CPEΔN, while Snail knockdown dramatically weakened interactions between CPEΔN with EZH2, HDAC1 and HDAC3 (**Figure 4C**).

The CPEΔN protein harbors a predicted HDAC interacting domain. To examine the domain in CPEΔN responsible for binding HDAC, we constructed three truncated proteins for co-immunoprecipitation assays: N-terminal CPEΔN N1 (1-118 aa) without the putative HDAC-interacting domain, CPEΔN N2 with the putative interacting domain (1-378 aa), and C-terminal truncated CPEΔN (379-440 aa) without the putative interacting domain. As shown in **Figure 4D**, CPEΔN N2 (1-378 aa) interacted with HDAC1, HDAC3 and Snail, while CPEΔN N1 (1-118 aa) and C-terminal CPEΔN (379-440 aa) did not, indicating that the binding domain of CPEΔN to HDACs and Snail is located within the region between 119 aa to 378 aa.

Taken together, these findings suggested that CPEΔN forms a complex with Snail, HDAC1, HDAC3 and EZH2 and that Snail is the core of the complex and recruits EZH2.

CPEΔN stabilizes the binding of Snail with EZH2

EZH2 is the catalytic subunit of polycomb repressive complex 2 (PRC2), which methylates Lys-9 and Lys-27 on histone 3 and represses gene expression [29]. Previous studies reported that Snail recruits HDACs and EZH2 to the *CDH1* promoter to reduce acetylation and increase trimethylation at H3K27 and H3K9 [30, 31]. To explore the functional role of CPEΔN in the HDAC1/HDAC3/Snail/EZH2 complex, we knocked down CPEΔN in H1395 cells. As shown in **Figure 4E**, the interaction of Snail with EZH2 was weakened in siCPEΔN cells, although the binding of HDAC1/HDAC3 with Snail was not affected. These finding suggested that the CPEΔN stabilizes the binding between Snail and EZH2.

HDAC1 deacetylase activity regulates complex assembly of CPE/Snail/HDAC/EZH2

Next, we assessed whether HDAC deacetylase activity affected the assembly of the CPEΔN/HDAC1/HDAC3/Snail/EZH2 complex. HDAC1 or HDAC3 inhibitors (TSA or RGFP966, respectively) were used to treat 95D or H1395 cells, and the CPEΔN/HDAC1/HDAC3 complex was analyzed. As shown in **Figure 4F** and **4G**, after 24 h of treatment with 300 nM of TSA, the binding of CPEΔN with EZH2 was almost undetectable. In contrast, the HDAC3 inhibitor RGFP966 did not affect EZH2 interaction with the complex. These results suggest that the deacetylase activity of HDAC1 plays a key regulatory role in EZH2 recruitment as well as in maintaining the stability of the CPEΔN/HDAC1/HDAC3/Snail/EZH2 complex.

To confirm these findings, ChIP-PCR experiments were performed. We first found that in H1395 cells with siRNA-mediated knockdown of CPEΔN, binding of EZH2 to the promoter region of *CDH1* was weakened (**Figure 3E**). We further found that after siRNA-mediated down-regulation of Snail in CPEΔN-H1299 cells, the binding activities of HDAC1, CPE, and EZH2 to the *CDH1* promoter declined by 30%, 50%, 73%, respectively, compared with the control group (**Figure 3F**). This result suggests that Snail is necessary for the binding of CPEΔN and EZH2 to the *CDH1* promoter. Finally, in CPEΔN-H1299 cells treated with TSA, the binding of EZH2, Snail and CPEΔN to the promoter region of *CDH1* was significantly decreased (**Figure 3G**), verifying that the interaction among these proteins relies on histone modification.

We further found that CPEΔN overexpression increased H3K27 and H3K9 trimethylation lev-

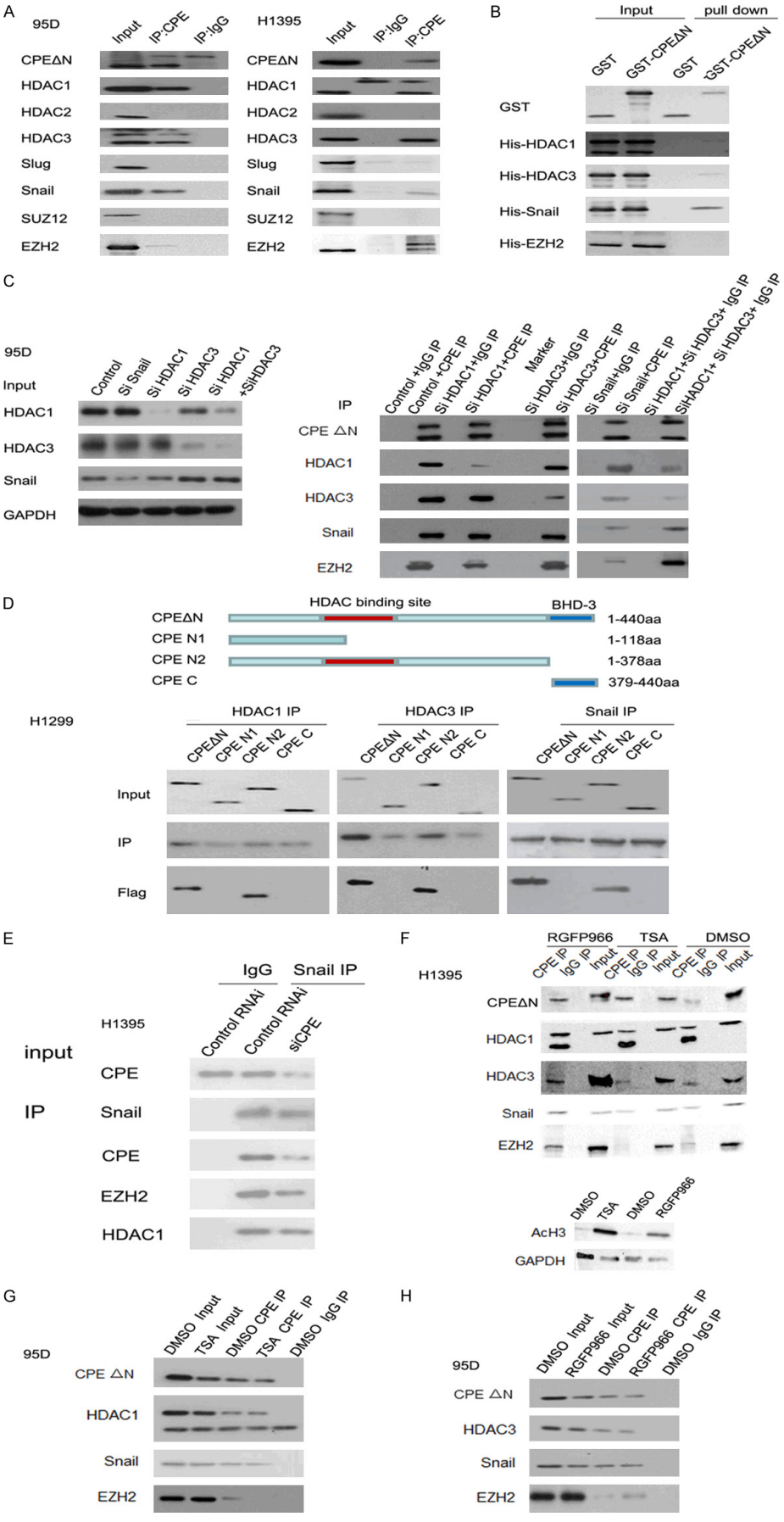
A
95D
Input
IP:CPE
IP:IgG
CPEΔN
HDAC1
HDAC2
HDAC3
Slug
Snail
SUZ12
EZH2
H1395
Input
IP:IgG
IP:CPE
B
Input
pull down
GST
GST-CPEΔN
GST-CPEΔN
His-HDAC1
His-HDAC3
His-Snail
His-EZH2
C
95D
Input
Control
Si Snail
Si HDAC1
Si HDAC3
Si HDAC1 +SiHDAC3
HDAC1
HDAC3
Snail
GAPDH
IP
Control +IgG IP
Control +CPE IP
Si HDAC1+IgG IP
Si HDAC1+CPE IP
Marker
Si HDAC3+IgG IP
Si HDAC3+CPE IP
Si Snail+IgG IP
Si Snail+CPE IP
Si HDAC1+Si HDAC3+ IgG IP
SiHADC1+ Si HDAC3+ IgG IP
CPE ΔN
HDAC1
HDAC3
Snail
EZH2
D
HDAC binding site
BHD-3
CPEΔN
CPE N1
CPE N2
CPE C
1-440aa
1-118aa
1-378aa
379-440aa
H1299
HDAC1 IP
HDAC3 IP
Snail IP
CPEΔN
CPE N1
CPE N2
CPE C
Input
IP
Flag
E
IgG
Snail IP
H1395
Control RNAi
Control RNAi
siCPE
input
CPE
IP
Snail
CPE
EZH2
HDAC1
F
H1395
RGFP966
TSA
DMSO
CPE IP
IgG IP
Input
CPEΔN
HDAC1
HDAC3
Snail
EZH2
DMSO
TSA
DMSO
RGFP966
AcH3
GAPDH
G
95D
DMSO
Input
TSA
Input
DMSO CPE IP
TSA
CPE IP
DMSO
IgG IP
CPE ΔN
HDAC1
Snail
EZH2
H
95D
DMSO
Input
RGFP966
Input
DMSO CPE IP
RGFP966
CPE IP
DMSO
IgG IP
CPE ΔN
HDAC3
Snail
EZH2

Figure 4. CPEΔN interacts with HDAC1, HDAC3, Snail and EZH2. A. Co-immunoprecipitation was performed in 95D and H1395 lung cancer cells. Candidate interacting proteins for CPEΔN were analyzed. B. Binding between GST-CPEΔN and His-tagged HDAC1, HDAC3, Snail and EZH2 *in vitro* was analyzed by GST pull-down assays. C. 95D cells were transfected with siRNAs as indicated. After 72 h, anti-CPE antibody was used to perform immunoprecipitation in cell lysates, and co-precipitation of HDAC1, HDAC3, Snail and EZH2 was detected. D. H1299 cells were transfected with plasmids expressing FLAG-CPEΔN, CPEΔN N1, CPEΔN N2 or CPEΔN C-terminal. After 36 h, the cells were lysed and immunoprecipitation was performed with anti-FLAG antibody; binding of CPEΔN truncations to HDAC1, HDAC3 and Snail was analyzed. E. H1395 cells were transfected with control siRNA or siCPE. After 72 h, anti-Snail antibody was used to perform immunoprecipitation, and co-precipitation of HDAC1, CPE and EZH2 was examined. F. H1395 cells were treated with DMSO, 300 nM TSA (HDAC1/HDAC2 inhibitor) or 10 mM RGFP966 (HDAC3 inhibitor) for 24 h; anti-CPE antibody or normal IgG antibody was used for immunoprecipitation, and co-precipitation of HDAC1, HDAC3, Snail, EZH2 was analyzed. G. 95D cells were treated with DMSO or 300 nM TSA for 24 h; anti-CPE or normal IgG antibody was used for immunoprecipitation, and co-precipitation of HDAC1, Snail, EZH2 was analyzed. H. 95D cells were treated with DMSO or 10 mM RGFP966 for 24 h; anti-CPE antibody or normal IgG antibody was used for immunoprecipitation, and co-precipitation of HDAC3, Snail, EZH2 was analyzed.

els and reduced H3K9 acetylation in both H1299 and H1975 cells (**Figure 3H**). These findings suggested that CPEΔN may regulate histone modification at the genome-wide scale and *CDH1*, might not be the only target gene regulated by CPEΔN. The pattern of CPEΔN suppressing *CDH1* expression is shown in **Figure 6**.

CPE levels are negatively correlated with E-cadherin expression in lung cancer tissues

To assess the correlation between the expression of CPEΔN and E-cadherin in lung cancer, we performed immunohistochemistry in a tissue microarray containing 75 lung adenocarcinoma samples as well as in 120 paraffin embedded samples of lung adenocarcinoma. Our previous study showed that both full-length and CPEΔN were expressed in lung adenocarcinoma, and CPEΔN was mainly located in the nucleus [9]. To eliminate the interference of full-length CPE, we specifically analyzed CPEΔN expression in the nucleus and found that expression levels of CPEΔN in the nucleus were significantly associated with disease stage and distant metastasis of lung adenocarcinoma (**Figure 5A-E**). CPEΔN expression in the nucleus showed a significant negative correlation with E-cadherin expression in the cell membrane (P=0.0166) (**Figure 5F** and **5G**). Lee et al reported that CPEΔN was only expressed in hepatocellular carcinoma, so we examined the expression of CPEΔN in hepatocellular carcinoma tissues as a positive control (in Supplementary Figure 3). The nuclear expression of CPEΔN was also negatively correlated with E-cadherin in a tissue microarray containing 205 samples of hepatocellular carcinoma (P=0.0129). The associations of CPE expression and clinicopathological characteristics of cancers are summarized in Supplementary Tables 2 and 3. These data indicate that CPEΔN expression is negatively correlated with E-cadherin in lung adenocarcinoma.

Discussion

In the present study, we have demonstrated that CPEΔN promoted cancer migration and invasion by repressing *CDH1* transcription. Upregulation of CPEΔN expression resulted in increased trimethyl modification at H3K9 and H3K27 in the *CDH1* promoter by 4-5-fold, while acetylation modification was significantly decreased. Immunoprecipitation mass spectrometry showed that potential CPEΔN-interacting proteins were primarily involved in transcription extension or epigenetic modification. We further found that CPEΔN binds to HDAC1, HDAC3 and Snail through a specific domain located within its intermediate region (119-378 aa). Together results suggest that CPEΔN may stabilize the Snail/HDAC/EZH2 complex and function as repressor of *CDH1* gene transcription.

The zinc finger protein Snail encoded by the *SNAI1* gene is a transcription factor that plays an essential role in regulating the metastasis and invasion of cancer cells. Snail binds to E-boxes in the promoter of *CDH1* and recruits HDAC1, HDAC2 and EZH2 to repress gene transcription [16]. Here we describe a novel mechanism in which CPEΔN enhances the interaction between Snail and EZH2. A recent study reported that the lncRNA HOTAIR promoted EMT by mediating the physical interaction between Snail and EZH2 [32]. Hepatitis C virus core protein, a molecule involved in hepatocarcinogenesis, was shown to reduce E-cadherin expression by stabilizing the interaction between Snail

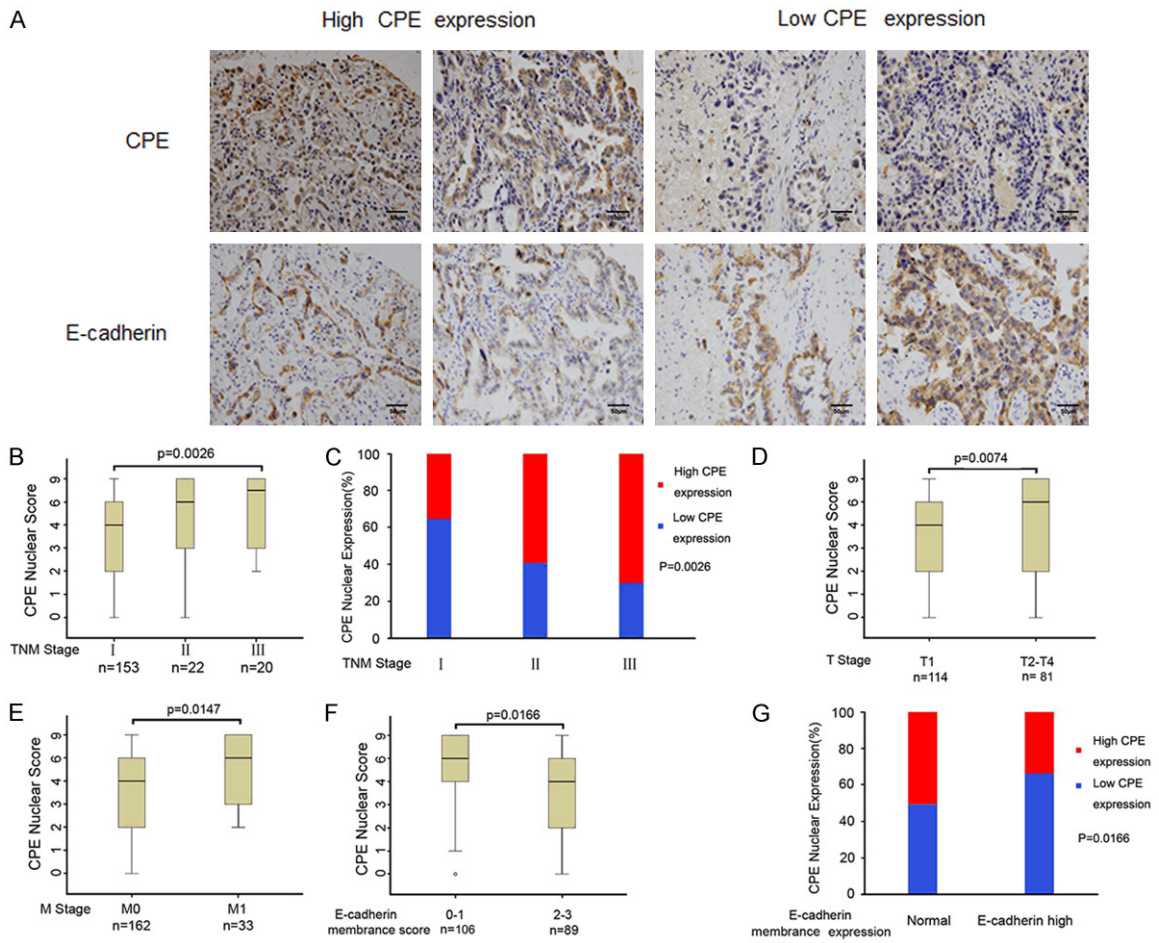

Figure 5. Nuclear expression of CPEΔN is negatively correlated with the cell membrane expression of E-cadherin in lung adenocarcinoma tissues. (A) The expression of CPE and E-Cadherin in a tissue microarray with 75 lung adenocarcinoma cases and 120 lung adenocarcinoma cases in paraffin slices were analyzed by immunohistochemical staining. Scale bars, 50 μm. (B) Box plot of CPE nuclear expression in lung adenocarcinoma tumors of different TNM stages. (C) A CPE staining score ≤6 was defined as low CPE expression, while a score >6 reflected high CPE expression. As described in (B), percentages of high CPE nuclear expression in the patient groups with different TNM stages were analyzed by the chi-square test. (D and E) Box plot of CPE nuclear expression in lung adenocarcinoma tumors of different T and M stages. Data were analyzed by the chi-square test. (F) The correlation between nuclear CPE expression and membrane E-cadherin expression was determined by Pearson's correlation. Outliers are marked with a circle. (G) Percentages of nuclear CPE expression in different E-cadherin membrane expression groups as shown in (F).

and HDAC1/HDAC2 [33]. Based on the current findings, we propose that stabilizing the Snail/HDAC/EZH2 complex might be a common mechanism used by various cancer-related factors to suppress the expression of E-cadherin and consequently promote cancer metastasis and progression. Thus, CPEΔN may be a novel target to interfere with the regulation of E-cadherin and therefore cancer progression in lung cancer cells.

In summary, we verified a positive correlation between high expression of CPEΔN with poor prognosis in patients with lung cancer and propose a model by which CPEΔN promotes cancer cell progression by suppressing the gene expression of E-cadherin through stabilizing the Snail/HDAC/EZH2 complex at the *CDH1* gene promoter. These findings suggest that CPEΔN may be a potential therapeutic target for lung cancer.

Acknowledgements

We would like to thank Professor Li Feng of China Medical University for assisting with in vivo imaging of mice and Professor Sun Wei of Beijing Protein Research Center for help with immunoprecipitation mass spectrometry. We are also grateful to Professor Yong Zhang of

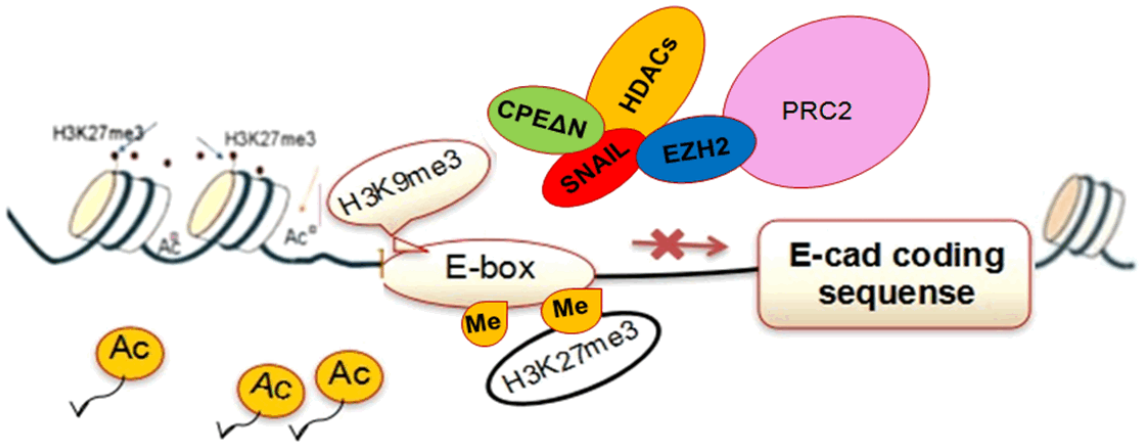

Figure 6. Schematic model of the proposed molecular mechanism by which the CPEΔN/HDAC1/HDAC3/Snail/EZH2 complex suppresses the *CDH1* promoter.

the Department of Pathology of the Liaoning Cancer Hospital for guidance in interpreting the pathological findings. This work was supported by the National Natural Science Foundation (81372287,81872363,81573654 and 81602407), the Key Project of Science and Technology of Liaoning province (20180551166 and 20170540565), the Guangdong Province Natural Science Foundation (2016A030313603), and the Key Project of Science and Technology of Shenyang (1801125).

Disclosure of conflict of interest

None.

Address correspondence to: Haozhe Piao, Central Laboratory, Cancer Hospital of China Medical University, Liaoning Cancer Hospital & Institute, Shenyang 110042, Liaoning, China. Tel: +86-024-31916626; E-mail: piaohaozhe1@126.com; Jimin Bao, Department of Otolaryngology Head and Neck Surgery, Liaoning Provincial Jinqiu Hospital, Shenyang 110016, Liaoning, China. E-mail: nose_bao@sohu.com

References

[1] Torre LA, Bray F, Siegel RL, Ferlay J, Lortet-Tieulent J and Jemal A. Global cancer statistics 2012. CA Cancer J Clin 2015; 65: 87-108.

[2] Chen W, Zheng R, Baade PD, Zhang S, Zeng H, Bray F, Jemal A, Yu XQ and He J. Cancer statistics in China 2015. CA Cancer J Clin 2016; 66: 115-32.

[3] Cool DR, Normant E, Shen F, Chen HC, Pannell L, Zhang Y and Loh YP. Carboxypeptidase E is a regulated secretory pathway sorting receptor: genetic obliteration leads to endocrine disorders in Cpe(fat) mice. Cell 1997; 88: 73-83.

[4] Cawley NX and Wetsel WC. New roles of carboxypeptidase E in endocrine and neural function and cancer. Endocr Rev 2012; 33: 216-53.

[5] Cheng Y, Cawley NX and Loh YP. Carboxypeptidase E (NF-α1): a new trophic factor in neuroprotection. Neurosci Bull 2014; 30: 692-6.

[6] Ji L, Wu HT, Qin XY and Lan R. Dissecting carboxypeptidase E: properties, functions and pathophysiological roles in disease. Endocr Connect 2017; 6: R18-R38.

[7] Sapio MR and Fricker LD. Carboxypeptidases in disease: insights from eptidomic studies. Proteomics Clin Appl 2014; 8: 327-37.

[8] Mitka M. Researchers discover new biomarker that may improve cancer care strategies. JAMA 2011; 305: 1184-5.

[9] Sun J, Meng D, Li L, Tian X, Jia Y, Wang H, Yu H, Sun T, Qu A, Shen H, Bao J and Zhang G. N-terminal truncated carboxypeptidase E expression is associated with poor prognosis of lung adenocarcinoma. Oncol Lett 2016; 12: 4659-4664.

[10] Zhou K, Liang H, Liu Y, Yang C, Liu P and Jiang X. Overexpression of CPE-ΔN predicts poor prognosis in colorectal cancer patients. Tumour Biol 2013; 34: 3691-9.

[11] Skalka N, Caspi M, Caspi E, Loh YP and Rosin-Arbesfeld R. Carboxypeptidase E: a negative regulator of the canonical Wnt signaling pathway. Oncogene 2013; 32: 2836-47.

[12] Wong SHM, Fang CM, Chuah LH, Leong CO and Ngai SC. E-cadherin: its dysregulation in carcinogenesis and clinical implications. Crit Rev Oncol Hematol 2018; 121: 11-22.

[13] Behrens J. Cadherins and catenins: role in signal transduction and tumor progression. Cancer Metastasis Rev 1999; 18: 15-30.
[14] Matějka VM, Fínek J and Králíčková M. Epithelial-mesenchymal transition in tumor tissue and its role for metastatic spread of cancer. Klin Onkol 2017; 30: 20-27.
[15] Serrano-Gomez SJ, Maziveyi M and Alahari SK. Regulation of epithelial mesenchymal transition through epigenetic and post-translational modifications. Mol Cancer 2016; 15: 18.
[16] Chiang C and Ayyanathan K. Characterization of the E-box binding affinity to snag-zinc finger proteins. Mol Biol (Mosk) 2012; 46: 907-14.
[17] Herranz N, Pasini D, Díaz VM, Francí C, Gutierrez A, Dave N, Escrivà M, Hernandez-Muñoz I, Di Croce L, Helin K, García de Herreros A and Peiró S. Polycomb complex 2 is required for E-cadherin repression by the Snail1 transcription factor. Mol Cell Biol 2008; 28: 4772-81.
[18] Yang X, Li L, Huang Q, Xu W and Cai X. Wnt signaling through Snail1 and Zeb1 regulates bone metastasis in lung cancer. Am J Cancer Res 2015; 5: 748-55.
[19] Peng L and Zhong X. Epigenetic regulation of drug metabolism and transport. Acta Pharm Sin B 2015; 5: 106-12.
[20] Smith E and Shilatifard A. Enhancer biology and enhanceropathies. Nat Struct Mol Biol 2014; 21: 210-9.
[21] Ehara H, Yokoyama T, Shigematsu H, Yokoyama S, Shirouzu M and Sekine SI. Structure of the complete elongation complex of RNA polymerase II with basal factors. Science 2017; 357: 921-924.
[22] Crickard JB, Lee J, Lee TH and Reese JC. The elongation factor Spt4/5 regulates RNA polymerase II transcription through the nucleosome. Nucleic Acids Res 2017; 45: 6362-6374.
[23] Qiu Y and Gilmour DS. Identification of regions in the Spt5 subunit of DRB sensitivity-inducing factor (DSIF) that are involved in promoter-proximal pausing. J Biol Chem 2017; 292: 5555-5570.
[24] Fitz J, Neumann T and Pavri R. Regulation of RNA polymerase II processivity by Spt5 is restricted to a narrow window during elongation. EMBO J 2018; 37.
[25] Carter CL, Lin C, Liu CY, Yang L and Liu ZR. Phosphorylated p68 RNA helicase activates Snail1 transcription by promoting HDAC1 dissociation from the Snail1 promoter. Oncogene 2010; 29: 5427-5436.
[26] Xia R, Jin FY, Lu K, Wan L, Xie M, Xu TP, De W and Wang ZX. SUZ12 promotes gastric cancer cell proliferation and metastasis by regulating KLF2 and E-cadherin. Tumour Biol 2015; 36: 5341-51.
[27] Tien CL, Jones A, Wang H, Gerigk M, Nozell S and Chang C. Snail2/Slug cooperates with Polycomb repressive complex 2 (PRC2) to regulate neural crest development. Development 2015; 142: 722-31.
[28] Hu J, Su P, Jiao M, Bai X, Qi M, Liu H, Wu Z, Sun J, Zhou G and Han B. trps1 suppresses breast cancer epithelial-mesenchymal transition program as a negative regulator of SUZ12. Transl Oncol 2018; 11: 416-425.
[29] Zhao K, He J, Wang YF, Jin SD, Fan Y, Fang N, Qian J, Xu TP and Guo RH. EZH2-mediated epigenetic suppression of EphB3 inhibits gastric cancer proliferation and metastasis by affecting E-cadherin and vimentin expression. Gene 2019; 686: 118-124.
[30] Oh JY, Choi GE, Lee HJ, Jung YH, Ko SH, Chae CW, Kim JS, Kim SY, Lim JR, Lee CK and Han HJ. High glucose-induced reactive oxygen species stimulates human mesenchymal stem cell migration through snail and EZH2-dependent E-cadherin repression. Cell Physiol Biochem 2018; 46: 1749-1767.
[31] Tong ZT, Cai MY, Wang XG, Kong LL, Mai SJ, Liu YH, Zhang HB, Liao YJ, Zheng F, Zhu W, Liu TH, Bian XW, Guan XY, Lin MC, Zeng MS, Zeng YX, Kung HF and Xie D. EZH2 supports nasopharyngeal carcinoma cell aggressiveness by forming a co-repressor complex with HDAC1/HDAC2 and Snail to inhibit E-cadherin. Oncogene 2012; 31: 583-94.
[32] Yang G, Shen T, Yi X, Zhang Z, Tang C, Wang L, Zhou Y and Zhou W. Crosstalk between long non-coding RNAs and Wnt/β-catenin signalling in cancer. J Cell Mol Med 2018; 22: 2062-2070.
[33] Nie D, Shan X, Nie L, Duan Y, Chen Z, Yang Y, Li Z, Tian L, Gao Q, Shan Y and Tang N. Hepatitis C virus core protein interacts with Snail and histone deacetylases to promote the metastasis of hepatocellular carcinoma. Oncogene 2016; 35: 3626-35.
[34] Lash RH and Genta RM. Routine anti-helicobacter immunohistochemical staining is significantly superior to reflex staining protocols for the detection of helicobacter in gastric biopsy specimens. Helicobacter 2016; 21: 581-585.

Supplementary Materials and Methods

Cell culture and cell migration assays

The cancer cell lines were obtained from ATCC and Chinese Academy of Sciences Cell Bank, and cultured at 37°C in an atmosphere containing 5% CO_2 in DMEM or 1640 medium supplemented with 5 or 10% fetal bovine serum (FBS).

Cell motility was analyzed by the scratch test. 95D cells in a 6-well plate were cultured to the logarithmic growth phase, and a 200 μl pipette tip was used for scratching. Fresh culture medium was used to wash out floating cells, and cells were imaged at 0 and 24 hours, respectively.

For cell migration and invasion assays, Transwell chambers were placed in a 24-well plate, and culture medium with 30% FBS was added to lower chambers. The top chambers included untreated 95D cells or their counterparts treated with siRNA, si-CPEΔN1 or si-CPEΔN2; about 5×10^5 cells were placed in each well and cultured at 37°C, in presence of 5% CO_2 and saturated humidity. After 24 hours of incubation, paraformaldehyde was used to fix cells, and crystal violet was employed for staining; finally, cells were imaged and counted. To confirm whether CPEΔN promoted the migration of lung cancer cells, control vector or CPEΔN was transfected into H1299 cells, respectively. After 24 hours of incubation, the cells were digested with pancreatin to single cell suspension; 5×10^5 cells were seeded into transwell chambers and incubated for 24 hours at 37°C, with 5% CO_2 and saturated humidity, and clone counting and imaging were carried out. The assay was independently repeated at least three times.

Construction of expression vectors

The human full length CPE, HDAC1, HDAC3, Snail and EZH2 gene templates were purchased from Hui Jun Gen Company (Guangzhou, China). CPEΔN was cloned into the pCMV-Flag and pGEX-4T-1 (Amersham) vectors, respectively, which were used for interaction assays in vivo and in vitro. The N1 (1-118 aa), N2 (1-378 aa) and C-terminal (379-440 aa) variants of CPEΔN were cloned into the pCMV-Flag vector, respectively, and used for coimmunoprecipitation to determine the interaction region of CPEΔN with HDACs, including Snail. CPEΔN was cloned into the pLenti-CMV-MCS-HA-3Flag-P2A-LUC vector, and the luciferase-CPEΔN fusion protein was used to screen stable lung cancer cell lines with CPEΔN overexpression for in vivo imaging experiments in mice. The HDAC1, HDAC3, Snail and EZH2 genes were cloned into the PET-28a(+) vector, and His labeled target proteins were bacterially expressed and used in GST-pull down assays for in vitro binding analysis. All PCR primers are shown in Supplementary Table 4.

Real time PCR

Trizol was used for total RNA extraction. Superscript III First Strand Synthesis System (Invitrogen total) was used for reverse transcription. Quantitative PCR was performed on an Exicycler 96 System in 25 μl reactions containing SYBR Green PCR master mix. Primers for specific genes are described in Supplementary Table 4. Quantitative PCR data were normalized to human GAPDH expression. Averages from at least three independent experiments are shown. *P* values were calculated between control and samples by Student's *t* test.

Western blot

Cell lysates were separated by 8-12% SDS-PAGE and transferred onto a polyvinylidene difluoride membrane (Millipore). After blocking with a 5% fat-free milk solution, the proteins of interest were detected with respective primary and HRP-conjugated secondary (Zhongshan Jinqiao Biosciences; 1:20000) antibodies. The primary antibodies used were: anti-CPE (1:1000; BD Biosciences #610758), anti-E-cadherin (1:2000; Cell Signaling #3195), anti-HDAC1 (1:4000; Abcam #ab7028), anti-HDAC3 (1:4000; Abcam #ab7030), anti-Snail (1:1000; Santa Cruz #sc10432), anti-EZH2 (1:1000; Millipore #17-662), anti-SUZ12 (1:1000; Proteintech #20366-1-AP), anti-Slug (1:1000; GenaTex #GTX121924), anti-HDAC2 (1:1000; Abcam #ab16032), anti-GAPDH (1:1000; Cell signaling #5174), anti-H3K27Ac (1:1000; Abcam

#ab45173), anti-H3K27Me3 (1:1000; #Ab92985), anti-H3K9Ac (1:1000; #ab32129), anti-H3K9Me3 (1:1000; #Ab176916), anti-H3K4Me3 (1:1000; #Ab12209), anti-H3K36Me3 (1:1000; #Ab9050), anti-acetyl Histone H3 (1:1000; Upstate #06-599), anti-α-catenin (1:1000; #Ab176916), anti-β-catenin (1:1000; #BD610153) and anti-γ-catenin (1:500; Immunoway #YT0678). Blots were developed with enhanced chemiluminescence (ECL) reagent (Thermo) and scanned on a ChemiDoc MP imager (Bi0-Rad).

RNA interference

The siRNA sequences used in this study are listed in Supplementary Table 4. The siRNAs were synthesized by Shang Hai GenePharm and transfected with Lipofectamine RNAi MAX (Invitrogen). Interference efficiency was evaluated by Western blot.

Supplementary Table 1. The suspected interacting proteins of CPEΔN were obtained by immunoprecipitation-tandem mass spectrometry from nuclear extracts of the CPEΔN-H1299 cells

Suspected interacting proteins	Sequence	Start position	End position
sp|O00267|SPT5H_HUMAN	ATAISLMR	191	198
sp|O00267|SPT5H_HUMAN	DNELIGQTVR	702	711
sp|O00267|SPT5H_HUMAN	DPNLWTVK	176	183
sp|O00267|SPT5H_HUMAN	DTYLDTQVVGQTGVIR	990	1005
sp|O00267|SPT5H_HUMAN	DVTNFTVGGFAPMSPR	653	668
sp|O00267|SPT5H_HUMAN	ETFQVLNMYGK	556	566
sp|O00267|SPT5H_HUMAN	EVANLKPK	269	276
sp|O00267|SPT5H_HUMAN	FEGDTGLIVR	485	494
sp|O00267|SPT5H_HUMAN	FIAYQFTDTPLQIK	200	213
sp|O00267|SPT5H_HUMAN	ILSVDGNK	440	447
sp|O00267|SPT5H_HUMAN	LGYWNQQMVPIK	247	258
sp|O00267|SPT5H_HUMAN	MDLDEQLK	1067	1074
sp|O00267|SPT5H_HUMAN	QAIEGVGNLR	237	246
sp|O00267|SPT5H_HUMAN	RDNELIGQTVR	701	711
sp|O00267|SPT5H_HUMAN	SSVGETVYGGSDELSDDITQQQLLPGVK	148	175
sp|O00267|SPT5H_HUMAN	TPAQSGAWDPNNPNTPSR	814	831
sp|O00267|SPT5H_HUMAN	TPMYGSQTPLQDGSR	784	798
sp|O00267|SPT5H_HUMAN	TPMYGSQTPMYGSGSR	768	783
sp|O00267|SPT5H_HUMAN	VVSISSEHLEPITPTK	1022	1037
sp|P16870|CBPE_HUMAN	EGGPNNHLLK	204	213
sp|P16870|CBPE_HUMAN	LTASAPGYLAITK	421	433
sp|P16870|CBPE_HUMAN	SNAQGIDLNR	180	189
sp|P63272|SPT4H_HUMAN	ALETVPK	2	8
sp|Q6P1Q9|MET2B_HUMAN	AGSYPEGAPAILADK	2	16
sp|Q6P1Q9|MET2B_HUMAN	AGSYPEGAPAILADKR	2	17
sp|Q6P1Q9|MET2B_HUMAN	TQTPPVEENVTQK	152	164
sp|Q96IZ6|MET2A_HUMAN	AGSYPEGAPAVLADK	2	16
sp|Q96IZ6|MET2A_HUMAN	AGSYPEGAPAVLADKR	2	17
sp|P30876|RPB2_HUMAN	AGVSQVLNR	464	472
sp|P30876|RPB2_HUMAN	GPIQILNR	1065	1072
sp|P30876|RPB2_HUMAN	IVATLPYIK	256	264
sp|P30876|RPB2_HUMAN	VSGDDVIIGK	860	869

SPT5, Transcription elongation factor; CPEB, Carboxypeptidase E; SPT4, Transcription elongation factor; MET2B, Methyltransferase-like protein 2B; MET2A, Methyltransferase-like protein 2A; RPB2, DNA-directed RNA polymerase II subunit.

Supplementary Table 2. Distribution of CPE in lung cancer according to clinicopathological characteristics

Characteristics	Number	CPE low expression	CPE high expression	*p*
Gender				
Female	86	49	37	0.7086
Male	109	65	44	
Age				
≤60	80	44	36	0.3858
>60	116	71	45	
TNM stage				
I	153	99	54	0.0026**
II	22	9	13	
III	20	6	14	
T stage				
T1	114	76	38	0.0074**
T2-T4	81	38	43	
Nodal metastasis				
Negative	162	101	61	0.0147*
Positive	33	13	20	
E-cadherin expression				
Normal	89	44	45	0.0166*
E-cadherin loss	106	70	36	

*indicates significant difference (P<0.05), **indicates significant difference (P<0.01).

Supplementary Table 3. Distribution of CPE in HCC according to clinicopathological characteristics

Characteristics	Number	CPE low expression	CPE high expression	*p*
Gender				
Female	53	36	17	0.7770
Male	152	100	52	
Age				
≤60	163	107	56	0.6773
>60	42	29	13	
TNM stage				
I+II	87	57	30	0.8302
III	118	79	39	
T stage				
T1-T2	87	57	30	0.8302
T3-T4	118	79	39	
Grade/Differentiation				
I (well)	33	28	5	0.0098**
II (moderate)	131	87	44	
III (poor)	41	21	20	
Membrane E-cadherin expression				
Normal	121	72	49	0.0129*
E-cadherin loss	84	64	20	

*indicates significant difference (P<0.05), **indicates significant difference (P<0.01).

Supplementary Table 4. Primers and siRNAs involved in the study

Real-time PCR	Name	Sequence
α-catenin	Sense	5'-GCAGCAACCCTGGGAAGTG-3'
	Anti-sense	5'-GAATCCGCCAGCAGAGCAG-3'
β-catenin	Sense	5'-CATACAGGACTTGGGAGGT-3'
	Anti-sense	5'-GTTGTTGTTGCATTGGGGT-3'
γ-catenin	Sense	5'-TGACAAGGACGACATCACGG-3'
	Anti-sense	5'-CACTGGTTGGGCTGGTTGA-3'
E-cadherin	Sense	5'-GAACGCATTGCCACATACAC-3'
	Anti-sense	5'-TGGTGTAAGCGATGGCGGCA-3'
ChIP-PCR primer		
primer 1	Sense	5'-GTTGTTGTTGCATTGGGGT-3'
	Anti-sense	5'-GTTGTTGTTGCATTGGGGT-3'
primer 2	Sense	5'-GCCAATCAGCGGTACGGGG-3'
	Anti-sense	5'-GCGGGCTGGAGTCTGAACTGA-3'
siRNA		
CPEΔN	Sense	5'-GAGUGGUAGUGCUCACGAA-3'
	Anti-sense	5'-UUCGUGAGCACUACCACUC-3'
Snail	Sense	5'-CCACAGAAAUGGCCAUGGGAAGGCCUC-3'
	Anti-sense	5'-GAGGCCUUCCCAUGGCCAUUUCUGUGG-3'
HDAC1	Sense	5'-GCUCCUCUGACAAACGAAUTT-3'
	Anti-sense	5'-AUUCGUUUGUCAGAGGAGCTT-3'
HDAC3	Sense	5'-CCCAGCUGAACAACAAGAUTT-3'
	Anti-sense	5'-AUCUUGUUGUUCAGCUGGGTT-3'
Negative-control	Sense	5'-UUCUCCGAACGUGUCACGUTT-3'
	Anti-sense	5'-ACGUGACACGUUCGGAGAATT-3'
Construction of Expression Vectors		
pcDNA3.1-CPEΔN	Upstream primer	5'-CTGGCTAGCTCTAGACTCGAGGCCACCATGGCCGGGCGAGGGGGCAG-3'
	Downstream primer	5'-ATGGTCTTTGTAGTCGGATCCAAAATTTAAAGTTTCTGACATCATTTTC-3'
pcDNA3.1-CPEΔN N1	Upstream primer	5'-GACGGGAATTCATGAGGCGGCG-3'
	Downstream primer	5'-GGTCGGATCCATCTATTCCCTGGGCATTG-3'
pcDNA3.1-CPEΔN N2	Upstream primer	5'-TACAGGAATTCATGAGGCGGCG-3'
	Downstream primer	5'-GGACGGATCCCAGGTATAAGCAATC-3'
pcDNA3.1-CPEΔN C	Upstream primer	5'-GGCGGAATTCACCTTGAGCAGATACAC-3'
	Downstream primer	5'-CAGAGGATCCCGTTCCACCATTCCAT-3'
pLenti-Luc-CPEΔN	Upstream primer	5'-CGAGCTCAAGCTTCGAATTCGCCACCATGAGGCGGCGCCGGCG-3'
	Downstream primer	5'-TCATCCTTGTAGTCGGATCCAAAATTTAAAGTTTCTGACATCAT-3'
pGEX-4T-1-CPEΔN	Upstream primer	5'-CCGCGTGGATCCCCGGAATTCATGGCCGGGCGAGGGGGCAG-3'
	Downstream primer	5'-GTCACGATGCGGCCGCTCGAGTTAAAAATTTAAAGTTTCTGACATCATTTTC-3'
pET-28a-Snail	Upstream primer	5'-ATGGGTCGCGGATCCGAATTCATGCCGCGCTCTTTCCTC-3'
	Downstream primer	5'-GTGGTGGTGGTGGTGCTCGAGTCAGCGGGGACATCCTGAG-3'
pET-28a-HDAC1	Upstream primer	5'-ATGGGTCGCGGATCCGAATTCATGGCGCAGACGCAGGGC-3'
	Downstream primer	5'-GTGGTGGTGGTGGTGCTCGAGTCAGGCCAACTTGACCTCC-3'
pET-28a-HDAC3	Upstream primer	5'-ATGGGTCGCGGATCCGAATTCATGGCCAAGACCGTGGCCTATTTC-3'
	Downstream primer	5'-GTGGTGGTGGTGGTGCTCGAGTTAAATCTCCACATCGCTTTCC-3'
pET-28a-EZH2	Upstream primer	5'-CAGCAAATGGGTCGCGGATCCATGGGCCAGACTGGGAAG-3'
	Downstream primer	5'-GTGGTGGTGGTGGTGCTCGAGAGGGATTTCCATTTCTCTTTC-3'

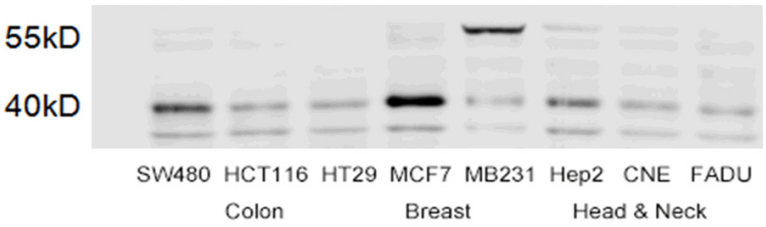

Supplementary Figure 1. Expression of the CPE protein in colon, breast, and head and neck cancer cell lines, detected by Western blot.

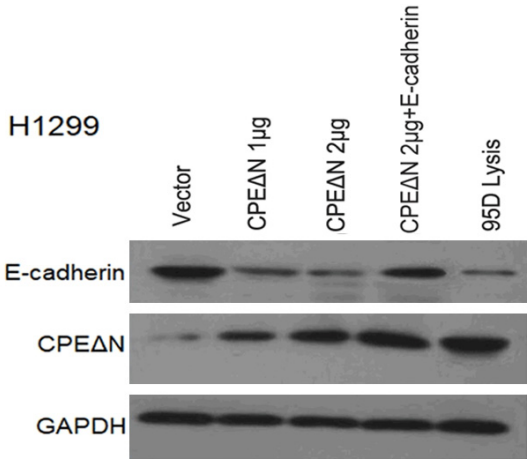

Supplementary Figure 2. The H1299 cells were transfected with empty vectors or different concentrations of CPEΔN plasmids or CPEΔN+E-cadherin plasmids, respectively. After 24 hours, the expression of CPEΔN and E-Cadherin was detected and GAPDH was used as internal reference.

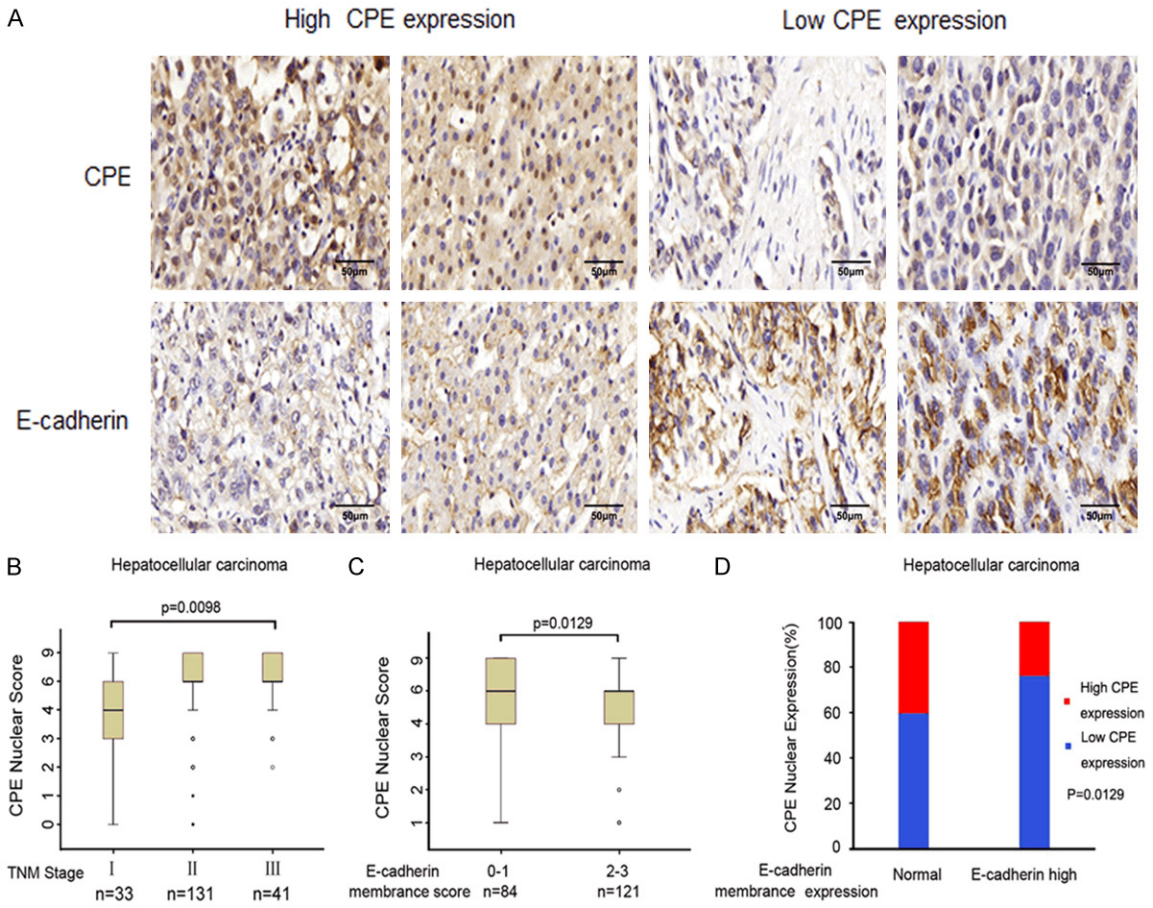

Supplementary Figure 3. The nuclear expression of CPEΔN is negatively correlated with the cell membrane expression of E-Cadherin in hepatocellular carcinoma tissues. (A) The expression of CPE and E-cadherin in hepatocellular carcinoma samples from 205 subjects were analyzed by immunohistochemical staining; scale bars, 50 μm. (B) Box plot of CPE expression in tumors of different TNM stages (I-III). Outliers are marked with a circle, and extreme cases are indicated by an asterisk. Data were analyzed by the chi-square test. (C) Box plot of nuclear CPE expression levels in hepatocellular carcinoma samples from 205 subjects. The subjects were divided into two groups based on E-cadherin membrane expression scores in the tumor: low scores, 0-1; high scores, 2-4. Data were analyzed by the chi-square test. (D) Percentages of nuclear CPE expression in different E-cadherin membrane expression groups as in (C).